Biochimica et Biophysica Acta, 1107 (1992) 165–174

BBAMEM 75653

Lipid–drug interaction: a structural analysis of pindolol effects on model membranes

Adriana Colotto [a,1], Paolo Mariani [a], Maria Grazia Ponzi Bossi [a], Franco Rustichelli [a], Gianni Albertini [b] and Lia Q. Amaral [c]

[a] *Istituto di Scienze Fisiche, Facoltà di Medicina, Ancona (Italy),* [b] *Dipartimento di Scienze dei Materiali e della Terra, Università di Ancona, Ancona (Italy) and* [c] *Instituto de Fisica, Universidade de Sao Paulo, São Paulo (Brazil)*

(Received 19 November 1991)

Key words: Lipid–drug interaction; X-ray diffraction; Calorimetry; Pindolol; Model membrane; Swelling

The ternary system constituted by distearoylphosphatidylcholine, pindolol (a vasodilator drug) and water has been investigated by using X-ray diffraction and calorimetric techniques. The structural modifications induced by the drug have been determined and a possible interaction model has been derived. In particular, the pindolol content–temperature dependent phase diagram shows the occurrence of two new phases: the first is an interdigitated gel, and the second is a lamellar structure presenting an unusual mixed disordered-ordered conformation of the hydrocarbon chains ($L_{\alpha\beta}$). The comparative analysis of electron density profiles relative to the $L_{\alpha\beta}$ phase, reveals significant modifications in the paraffinic region of the lipid layer. In agreement with thermodynamic results, the structural data suggest that the drug induces a stiffening and a tightening of the hydrocarbon chains. Moreover, the hydrophilic properties of the membrane (particularly in $P_{\beta'}$ and $L_{\alpha\beta}$ phases) present an evident dependence with the drug concentration.

1. Introduction

The pharmacokinetic behaviour is an important determinant in the therapeutic utility of a drug. In fact, to a great degree, both the desirable actions and undesirable side effects of drugs are governed by their concentration and persistence in the various body subcompartments. As the lipidic plasma membrane consists in an inevitable part of the route from the site of administration to the plasma compartment, there is an evident interest in getting as much information as possible on the interaction between drugs and membranes [1]. Moreover, it is believed that the interaction with the lipid constituents of membranes, resulting in an alteration of the fluidity, may be an important mode of action of some drugs [2–4].

On the other hand, due to the unique morphology and unusual transport properties of phospholipid bilayers, the use of liposomes as carriers for drugs and other biologically active substances has been largely explored. In particular, the capability of liposomes to simulate many of those properties of the living cell determined at the membrane level, increases still more the interest in this field [5]. In this context, the study of the alterations induced by drugs in model membranes, composed by a single lipid and water, has turned to be a common procedure.

In this work we report the results of a combined X-ray diffraction and calorimetric analysis of a model membrane system constituted of 1,2-distearoyl-3-phosphatidylcholine (DSPC) and water, when pindolol (a vasodilator drug widely used in heart treatments) is present. The ternary system has been studied firstly in fully hydrated conditions, for various drug concentrations. Significant changes in both thermodynamical and structural parameters were observed: in particular, the pindolol induces the appearance of an interdigitated 'gel' phase and a high temperature lamellar phase, which is unusually characterized by a mixed conformation of the lipid hydrocarbon chains. In order to fully characterize such structures, some representative pindolol concentrations have been considered, and the samples investigated as a function of water content.

2. Materials and Methods

2.1. Sample preparation

1,2-Distearoyl-3-phosphatidylcholine (DSPC) was purchased from Sigma (St. Louis, MO, USA) and was

[1] Present address: Institut für Röntgenfeinstrukturforschung, Steyrergasse, 17/VI, 8010 Graz, Austria.

Correspondence: P. Mariani, Istituto di Scienze Fisiche, Facoltà di Medicina, via Ranieri Monte d'Ago, 60131 Ancona, Italy.

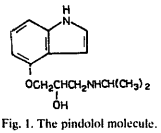

Fig. 1. The pindolol molecule.

used without further purification. Pindolol (99% purity (Fig. 1) was provided by the Pharmacology Institute of the University of Ancona, Italy. The melting of pure pindolol occurs at 172 °C.

Proper quantities of drug were added to the phospholipid according to the desired molar ratio R between pindolol and DSPC, ranging from 0 to 1. The mixtures were dissolved in chloroform, dried in nitrogen stream and lyophilized. Bidistilled water was then added in the desired weight concentrations.

Excess water samples were prepared with a water to DSPC weight ratio of 3. These aqueous mixtures were incubated for about 4 h at 65 °C, and vortexed several times for about 1 min. The water composition of the phase has been estimated by gravimetric analysis (see Table I). Not fully hydrated samples were prepared by adding water at the desired weight concentrations, and allowing the system to hydrate at room temperature for several days.

2.2. Calorimetry

Calorimetric measurements were performed using a Perkin-Elmer calorimeter, model DSC-2C with related data processor. A 2.5 C°/min scan rate was used both in the heating and cooling cycles. Aluminium containers of 20 μl were used. The calorimeter was standardized and calibrated using pure distilled water and n-octadecane [6]. Transition temperature were taken as the point of intersection between the tangent to the transition peak at its steepest point and the approximate extrapolated baseline. Transition enthalpies were determined from the peak area and are referring to the amount of lipid in the DSC pan, which has been estimated by gravimetric analysis considering the initial sample composition.

2.3. X-ray diffraction

Low-angle X-ray diffraction experiments were performed using a conventional X-ray generator (Cu-Kα radiation). A Guinier camera operating in vacuum with a bent quartz crystal monochromator (λ = 1.54 Å) and a cylindrical film cassette with diameter of 123 mm was used. The samples were located between two mica windows in a circular hole and were continuously rotated during exposure to avoid orientation effects. The temperature was controlled within ± 1C° by using a circulation thermostat. The diffraction patterns were recorded on a stack of four Kodak DAF-392 films. Densitometric traces of the films were obtained on a Enraf-Nonius Delst model II microdensitometer and the relative intensities of reflections were calculated as reported in Ref. 7. Unit cell dimensions were calculated from Bragg's equation.

High-angle X-ray diffraction patterns were obtained by using a powder diffractometer on a Rigaku Denki RV300 rotating anode generator. The sample holders and temperature control were the same described above for low-angle X-ray diffraction experiments.

TABLE I

Chemical composition and structural data: fully hydrated samples

All data refer to DSPC/water/pindolol mixtures in condition of maximum hydration, i.e., as close as possible to the fully hydration. C and $C_{v,wat}$ are the weight and volume concentrations of water, respectively. Volume concentrations have been calculated according to Ref. 13 using specific volumes of 0.958 cm^3/g for DSPC [7] and of 1 cm^3/g for both water and pindolol. d is the lamellar repeat distance, which corresponds to the total thickness of lipid and water layers, while d_{hp} is the thickness of the lipid layer only, calculated using $d_{hp} = d \cdot (1 - C_{v,wat})$ [13]. θ is the angle of tilt of the paraffinic chains with respect to the normal to the lamellae [11].

T = 25°C, $L_{\beta'}$ phase:					
R	C	$C_{v,wat}$	d (Å)	d_{hp} (Å)	θ (°)
0	0.30	0.309	67.9	46.9	40.0
0.01	0.30	0.308	69.4	48.0	38.6
0.05	0.30	0.306	74.2	51.5	32.9
T = 25°C, intermediate biphasic region:					
R	C	$C_{v,wat}$	$d_{L\beta'}$ (Å)	d_{gel} (Å)	
0.1	0.30	0.309	67.9	56.0	
0.2	0.30	0.308	66.0	54.2	
T = 25°C, gel phase:					
R	C	$C_{v,wat}$	d (Å)	d_{hp} (Å)	
0.4	0.35	0.330	54.9	36.8	
0.5	0.35	0.327	54.2	36.5	
0.5 [a]	0.30	0.277	52.0	37.6	
T = 52°C, $P_{\beta'}$ phase:					
R	C	$C_{v,wat}$	d (Å)	d_{hp} (Å)	θ (°)
0	0.33	0.339	74.0	48.9	37.2
0.1	0.35	0.353	77.4	50.0	35.4
0.5 [b]	0.37	0.345	77.8	50.9	33.9
T = 65°C, L_α and $L_{\alpha\beta}$ phases:					
R	C	$C_{v,wat}$	d (Å)	d_{hp} (Å)	
0	0.30	0.310	60.5	41.7	
0.05	0.31	0.319	61.0	41.5	
0.1	0.35	0.359	65.5	42.0	
0.2	0.35	0.359	65.8	42.2	
0.5	0.35	0.358	68.5	44.0	
0.8 [c]	0.40	0.408	77.4	45.8	

[a] The data correspond to a not fully hydrated sample.
[b] The sample temperature was 54 °C.
[c] Pindolol crystals were detected in this sample.

3. Study of pindolol effects on fully hydrated DSPC samples

3.1. Differential scanning calorimetry

Calorimetric measurements were performed as a function of the pindolol content on fully hydrated DSPC samples. The investigated temperature range was from 15°C to 70°C. As expected, the calorimetric curves relative to the reference sample ($R = 0$) show two characteristic endothermic peaks, corresponding to the so-called pre- and main-transitions [8]. Within the investigated pindolol concentration range, two endothermic peaks were still observed, indicating the persistence of the two phase transitions: however, their thermodynamical characteristics appear to change as a function of the drug content. In particular, the lower frame of Fig. 2 shows that both the transition temperatures slightly increase for drug concentrations higher than about 0.2. The maximum shift, about 5°C for the pre- and 3°C for the main-transition, is observed for $R = 0.8$. More evident effects concern the transition enthalpies (see the upper frame of Fig. 2). In particular, the pre-transition enthalpy significantly reduces

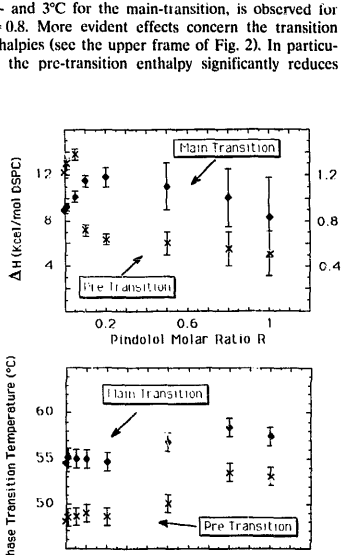

Fig. 2. Calorimetric data observed as a function of pindolol molar ratio ($R = mol_{pind}/mol_{DSPC}$) in fully hydrated DSPC/water mixtures. Lower part: transition temperature. Upper part: transition enthalpy (the scale in the left side is relative to the so-called main transition, and the one in the right refers to the pre-transition).

when the drug content exceeds the $R = 0.1$ value, while, on the contrary, the enthalpy associated to the second phase transition increases as a function of drug concentration, approaching a plateau, but softly decreases when R overtakes 0.5. It must be noticed, however, that enthalpy calculations for molar ratio higher than 0.5 are affected by very large errors, as samples contain not-negligible amounts of pindolol crystals (see also below).

Some indications arise from such results. At one hand, the presence of two phase transitions, which seem to maintain the same meaning of those observed in the pure DSPC/water system, indicates that low concentrations of pindolol do not alter the characteristic phase sequence. On the other side, the behaviour observed on the transition temperatures seems to indicate that pindolol does not show any fluidising effect on the membrane. Indeed, the small increase of the melting chain transition temperature and the effect on the enthalpy observed at higher drug concentrations may indicate that pindolol has actually a rigidifying effect.

3.2. X-ray diffraction

As well known, three different phases, namely the $L_{\beta'}$, $P_{\beta'}$ and L_α phases, are observed in the temperature dependent phase diagram of a fully hydrated DSPC/water system [9–12]. Such phases show a lamellar structure and are, respectively, characterized by a distorted pseudo-hexagonal, hexagonal and liquid-like arrangement of the hydrocarbon chains inside the layer [11,12]. Moreover, in the $P_{\beta'}$ phase, the lipid bilayers are distorted by a periodic ripple so that the structure presents a two-dimensional lattice. As usual in lipid crystallography, we refer in the following to two distinct regions of the X-ray scattering spectra, considering separately the low-angle pattern (2θ diffraction angles ranging from about 10′ to 10°) from the high-angle scattering (centered around a 2θ angle of about 20°). The first region gives information about the long-range organization of the structure elements and specifies the crystalline lattice and symmetry. The second region is related to the short range molecular organization and specifies the conformation of the hydrocarbon chains [11,13].

Concerning the present X-ray diffraction experiments, two peculiar points must be remarked. First, for drug molar ratios higher than about 0.6, and at all temperatures investigated, several very narrow peaks were detected in X-ray diffraction profiles. Considering their spacings, these peaks appear related to the presence of pindolol crystals, indicating that the drug is not fully disperse in lipids. Therefore, in this condition, the pindolol sample concentration does not correspond to the pindolol 'phase' concentration, so that a detailed crystallographic analysis appears meaningless.

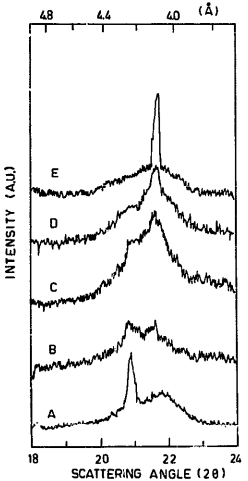

Fig. 3. High-angle X-ray diffraction profiles observed at 25°C for different pindolol molar ratio ($R = mol_{pind}/mol_{DSPC}$) in fully hydrated DSPC/water mixtures. A: $R = 0$; B: $R = 0.01$; C: $R = 0.05$; D: $R = 0.1$; E: $R = 0.4$. Note that the profiles show different scattering intensities, mainly due to the not perfect crystallinity of the samples.

Second, long times appeared necessary to reach 'equilibrium' conditions during sample preparation, as the phospholipids hydration in presence of high quantity of pindolol often resulted not homogenenous. Moreover, large hysteresis were detected during heating or cooling cycles, and in particular in correspondence with phase transitions, so that repeatable behaviours were obtained only with some difficulty.

3.2.1. High-angle scattering analysis. The hydrocarbon chains of a fully hydrated DSPC sample show at 25°C the so-called β' conformation: the chains are tilted with respect to the polar/apolar interface, stiff, fully elongated and packed in a quasi-hexagonal bidimensional lattice [11]. The corresponding high-angle X-ray diffraction profile is characterised by a sharp peak at 4.25 Å, and by a diffuse band centred at about 4.0 Å (Fig. 3, profile A). The addition of pindolol determines significant changes, as reported in Fig. 3. In particular, the sharp peak at 4.25 Å decreases in height and flattens, while the broad band becomes sharper (see for example the profiles B and D); when R overtakes 0.4, only a sharp peak, centered at about 4.1 Å, still remains (see the profile E). As already observed in other lipid-drug systems, the vanishing of the hydrocarbon chain tilt could explain this behaviour [14,15].

In the temperature range between the two phase transitions, the hydrocarbon chains of a fully hydrated DSPC sample still show the β' conformation [11]. However, as the chain packing is hexagonal, the diffraction profile presents only one symmetrical reflection [11], which, at 52°C, appears centered at about 4.2 Å. When pindolol is added, this pattern is modified. In particular, at concentration higher than $R = 0.4$, a shoulder appears in the high-angle side of the peak (at about 4.1 Å). Noticeable is the fact that its intensity presents a strong dependence on the drug concentration and temperature, being more and more visible as far as the pindolol content increases and disappearing when the temperature rises. This behaviour seems to indicate a coexistence of the β' conformation with an untilted chain arrangement.

The main transition corresponds to the melting of the chains, which assume a liquid-like α conformation [11]: in the case of a fully hydrated DSPC sample, the X-ray diffraction profile shows a single broad reflection, centered at 65°C at about 4.5 Å (see in Fig. 4 the profile A). The addition of pindolol in molar ratio higher than about 0.1, determines the appearance of a sharp reflection, centered at about 4.2 Å (profiles B and C in Fig. 4). The intensity of that sharp reflection appears strongly dependent on the drug concentration.

3.2.2. Low-angle scattering analysis. The low-angle diffraction pattern observed below the pre-transition temperature for a fully hydrated DSPC sample is char-

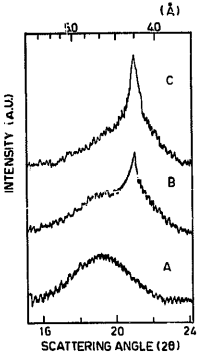

Fig. 4. High-angle X-ray diffraction profiles observed at 65°C for different pindolol molar ratio ($R = mol_{pind}/mol_{DSPC}$) in fully hydrated DSPC/water mixtures. A: $R = 0$; B: $R = 0.2$; C: $R = 0.5$.

acterised by several sharp peaks, the spacings of which clearly indicate a one-dimensional lamellar lattice (see Table II). According to the previously discussed high-angle profile, this phase is identified as $L_{\beta'}$ [11,12]. The addition of pindolol at molar ratios lower than 0.1 does not change this picture: however, the unit cell dimension as well as the lipid leaflet thickness (calculated as reported in Table I) appear to increase, confirming the possible occurrence of a gradual transition towards the β (untilted) chain conformation. In the intermediate range of the pindolol concentration, and in particular for R between 0.1 and 0.4, it was necessary to repeat the experiments several times, as the diffraction profiles showed the presence of some unindexable reflections. A careful analysis of data indicates finally that two different lamellar phases coexist in this concentration range, one having structural parameters compatible with the $L_{\beta'}$ phase and the other being characterised by a suprising small layer thickness (see Tables I and II).

When the drug molar ratio is equal to 0.5, the lamellar phase with relatively small unit cell is indeed observed pure (see Tables I and II). The layer periodicity is of about 52 Å, and appears not-compatible with the occurrence of a L_β phase. In fact, the above discussed high-angle diffraction pattern seems to indicate an untilted arrangement of hydrocarbon chains: however, the expected thickness of two apposing DSPC molecules with fully extended untilted chains is about 58 Å [11], i.e., already larger that the layer periodicity observed. We conclude that this phase is actually an interdigitate 'gel', namely a structure in which the phospholipid hydrocarbon chains, which are stiff, fully elongated and perpendicular to the lamellar planes, are interdigitated. The difference between the expected thickness of a lipid bilayer made of DSPC molecules with fully extended untilted chains (58 Å) and the lipid bilayer as determined from the sample concentration (about 37 Å, see Table I), is 21 Å, i.e., assuming 1.25 Å per CH_2 group, of about 17 CH_2 groups. This corresponds to an interpenetration of hydrocarbon chains up to the first CH_2 groups of the

TABLE II

Experimental data: indexing of reflections observed in fully hydrated samples at 25°C

S_{obs} is the reciprocal spacing of observed reflections, and S_{calc} is the value calculated considering a one-dimensional lamellar lattice, i.e., using $S_{calc} = h/d$, where d is the lattice parameter and h is the Miller index of the reflection. The underlined S values correspond to reflections not observed in the X-ray pattern. Other notations as in the text and Table I.

$R = 0.0$	$L_{\beta'}$ phase, $d = 67.9$ Å	
S_{obs} (10^{-3} Å^{-1})	h	S_{calc} (10^{-3} Å^{-1})
14.8	1	14.7
29.6	2	29.5
44.1	3	44.2
58.9	4	58.9
–	5	73.6

$R = 0.01$	$L_{\beta'}$ phase, $d = 69.4$ Å	
S_{obs} (10^{-3} Å^{-1})	h	S_{calc} (10^{-3} Å^{-1})
14.4	1	14.4
28.6	2	28.8
43.0	3	43.2
57.6	4	57.6
–	5	72.1

$R = 0.05$	$L_{\beta'}$ phase, $d = 74.2$ Å	
S_{obs} (10^{-3} Å^{-1})	h	S_{calc} (10^{-3} Å^{-1})
13.5	1	13.5
26.9	2	27.0
40.7	3	40.4
53.6	4	53.9
–	5	67.4

$R = 0.1$	$L_{\beta'}$ phase, $d = 67.9$ Å		Gel phase, $d = 56.0$ Å	
S_{obs} (10^{-3} Å^{-1})	h	S_{calc} (10^{-3} Å^{-1})	h	S_{calc} (10^{-3} Å^{-1})
14.6	1	14.7		–
18.0		–	1	17.9
29.6	2	29.5		–
35.4		–	2	35.7
44.2	3	44.2		–
–		–	3	53.6
59.2	4	58.9		–
–		–	4	71.4

$R = 0.2$	$L_{\beta'}$ phase, $d = 66.0$ Å		Gel phase, $d = 54.2$ Å	
S_{obs} (10^{-3} Å^{-1})	h	S_{calc} (10^{-3} Å^{-1})	h	S_{calc} (10^{-3} Å^{-1})
15.2	1	15.2		–
18.2		–	1	18.5
30.2	2	30.3		–
37.4		–	2	36.9
–	3	45.5		–
–		–	3	55.4
60.6	4	60.6		–
–		–	4	73.8

TABLE II (continued)

$R = 0.4$	Gel phase, $d = 54.9$ Å	
S_{obs} (10^{-3} Å^{-1})	h	S_{calc} (10^{-3} Å^{-1})
18.3	1	18.2
36.6	2	36.4
54.3	3	54.6
–	4	72.9

$R = 0.5$	Gel phase, $d = 54.2$ Å	
S_{obs} (10^{-3} Å^{-1})	h	S_{calc} (10^{-3} Å^{-1})
18.5	1	18.8
36.7	2	36.9
55.7	3	55.4
–	4	73.8

lipid of the apposing monolayer. It is interesting to note that similar gel phases were previously detected in many phospholipid/water systems containing drugs (see for example Ref. 14) or surface-active molecules [16].

Above the pre-transition temperature, the well known $P_{\beta'}$ lamellar phase is expected [11,12]. Once more, the addition of small quantities of pindolol seems not to modify dramatically the structure, even if the lamellar thickness gradually increases (at 52°C from 74.0 Å to 77.4 Å when R changes from 0 to 0.1). At the same temperature, when the drug molar ratio is larger than 0.3, an extented two-phase region is observed. According to the high-angle profiles, it possible to identify the two phases as the previously discussed interdigitated gel, which coexists with the $P_{\beta'}$ phase. However, and in agreement with the high-angle observations, the pure $P_{\beta'}$ phase can be still obtained slowly increasing the temperature. Nevertheless, the corresponding layer thickness appears unusually large (at 55°C, the $R = 0.5$ sample shows a repeat distance of about 77.8 Å). The structural data, as reported in Table I, indicate that the presence of pindolol decreases the lipid chain tilt but also modify the hydrophilic properties of the bilayer, as the water phase composition increases.

Above the main transition temperature, and for all the investigated pindolol concentrations (but, as previously discussed, pindolol crystals are detected for R higher than 0.5), the low-angle X-ray diffraction profile appears compatible with the presence of a pure lamellar phase. However, also in this case, the structural data are sensitive to the drug concentration (see Table I). The peculiar characteristics of the high angle pattern suggest that the hydrocarbon chains are in an intermediate conformation [17], i.e., partially in α and partially in a more ordered arrangement. Considering that the proportion of chains in the two conformations seems to change as a function of the drug content, we call this conformation $\alpha\beta$ [17]. Actually, the increase of the layer thickness observed as a function of pindolol concentration, could be directly related to the rigidifying effect on the paraffinic chain conformation.

A pictorial representation of the temperature – pindolol molar ratio dependent phase diagram is reported in Fig. 5. The presence of a large region of coexistence of two (or more) phases must be pointed out. Moreover, dots indicate the region where pindolol crystals were detected. In biphasic regions, the assignement of structures was in many cases unsuccessful, due to unresolved X-ray spectra and/or to the impossibility of attaining samples in thermodynamical equilibrium. For such reasons, the boundary lines which separate the different phases are to be considered only as largely approximated.

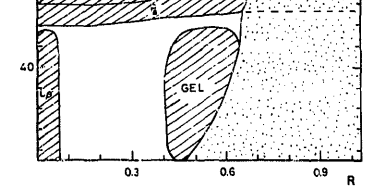

Fig. 5. Qualitative temperature – pindolol molar ratio ($R = mol_{pind}/mol_{DSPC}$) dependent phase diagram for fully hydrated DSPC/water mixtures. The one-phase regions are hatched. The dots indicate the region where pindolol crystals are present. The nomenclature and the structure of the phases are given in the text.

4. Structural analysis of the high temperature lamellar phase

In order to obtain further information on the lipid–drug interaction, three representative pindolol molar ratios were chosen (namely, $R = 0$, $R = 0.1$ and $R = 0.5$). In particular, after the determination of the respective temperature – water concentration phase diagrams, the low-angle diffracted intensities observed in the high temperature lamellar phase were measured and the corresponding electron density profiles calculated. For this purpose, and in order to solve the crystallographic phase problem, a so-called 'swelling' experiment was performed [18].

4.1. Phase diagrams

The temperature and water concentration dependent phase diagrams, traced for the two samples with 0.1 and 0.5 pindolol molar ratios, are reported in Fig. 6. For the same reasons just above discussed, these phase diagrams must be considered only qualitative.

Making reference to the phase diagrams of the DSPC/water system [11,12], where $L_{\beta'}$, $P_{\beta'}$ and L_α phases are present also for few percent of water, several comments appear necessary. It is evident that pindolol dramatically modifies the phase behaviour, inducing the appearance of the interdigitated 'gel' and $L_{\alpha\beta}$ phases. Besides, as the drug is practically not soluble in water, pindolol crystals are observed in the drier side of phase diagrams, in a region which appears more and more large as far as the drug concentration increases. Concerning the observed phases, the persistance of the $P_{\beta'}$ phase could be noticed, even if, as previously indicated (see Table I), some structural modifications seem to take place. Above the main-

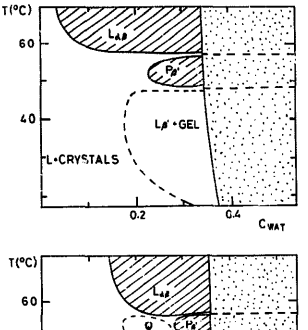

Fig. 6. Qualitative temperature – water concentration dependent phase diagrams for pindolol/DSPC mixtures having pindolol molar ratios ($R = mol_{pind}/mol_{DSPC}$) equal to 0.1 (upper diagram) and 0.5 (lower diagram). The one-phase regions are hatched. The dots indicate the region where the phases coexist with bulk water. The nomenclature and the structure of the phases are given in the text.

transition temperature, both phase diagrams show the $L_{\alpha\beta}$ phase. As discussed above, this phase presents a clear sensitivity to the pindolol content. Considering the structural and chemical data reported in Table III, it appears that pindolol induces a larger hydrophilicity of samples, as they saturate at higher water concentration (about 40% w/w instead of 30% [11,19], see Table III). It is also interesting to note that the thickness of the lipid leaflet decreases as a function of the water content. However, such a 'compression' effect appears balanced by the presence of pindolol, which acts stiffening the hydrocarbon chain organization: therefore, at the same water concentration, the sample containing the higher quantity of drug shows the larger lipid layer thickness.

As a final note, we remark that in the $R = 0.5$ sample, at about 50°C and for water concentrations ranging from about 15% to 20% (w/w), a coexistence of a one-dimensional lamellar phase (L or P) and of a not fully characterised more ordered phase Q (cubic?) was detected.

4.2. Swelling experiments

The intensity analysis was made within the regions of phase diagrams where the continuous transition from L_α to the $L_{\alpha\beta}$ phase seems to occur.

X-ray diffraction patterns give a set of integral intensities from which the module of the structure factors can be calculated. In the simple case of one-dimensional phases, the equation which gives the structure factors $F(h)$ reduces to:

$$F^2(h) = I(h)/m(h)$$

where h is the Miller index of the reflection, $I(h)$ is its observed intensity and $m(h)$ the multiplicity [20]. In order to solve the crystallographic 'phase problem', i.e., to determine the signs of the structure factors, it is traditional in lipid crystallography to perform swelling

TABLE III

Chemical composition and structural data: swelling experiments

The intensities of any experiment are normalised such that $\Sigma I(h) = 1.0$. The experimental error in measuring diffracted intensities is estimated to be ± 0.012. The d^*_{lip} are measured from the electron density maps (see text). Other notations as in the text and Table I.

$R = 0$					
C	0.10	0.17	0.26	0.30	(0.75)
$C_{v,wat}$	0.10	0.18	0.27	0.31	–
d (Å)	53.0	55.7	59.8	60.4	60.7
d_{lip} (Å)	47.5	45.9	43.8	41.7	–
d^*_{lip} (Å)	–	–	–	40.4	–
$I(1)$	0.609	0.563	0.489	0.482	–
$I(2)$	0.030	0.112	0.236	0.254	–
$I(3)$	0.100	0.185	0.210	0.203	–
$I(4)$	0.259	0.140	0.065	0.060	–
$I(5)$	0	0	0	0.112	–
$R = 0.1$					
C	0.08	0.15	0.20	0.35	(0.75)
$C_{v,wat}$	0.08	0.16	0.22	0.36	–
d (Å)	51.8	56.2	57.3	65.6	65.8
d_{lip} (Å)	47.5	47.4	44.9	42.0	–
d^*_{lip} (Å)	–	–	–	42.9	–
$I(1)$	0.819	0.809	0.718	0.475	–
$I(2)$	0.120	0.019	0.072	0.302	–
$I(3)$	0.032	0.005	0.026	0.083	–
$I(4)$	0.029	0.167	0.184	0.097	–
$I(5)$	0	0	0	0.043	–
$R = 0.5$					
C	0.20	0.25	0.30	0.35	(0.75)
$C_{v,wat}$	0.21	0.26	0.31	0.36	–
d (Å)	62.8	64.2	67.1	68.5	68.9
d_{lip} (Å)	49.9	47.7	46.4	44.0	–
d^*_{lip} (Å)	–	–	–	45.2	–
$I(1)$	0.720	0.559	0.468	0.370	–
$I(2)$	0.079	0.185	0.331	0.380	–
$I(3)$	0.055	0.066	0.082	0.069	–
$I(4)$	0.146	0.107	0.077	0.124	–
$I(5)$	0	0.028	0.042	0.057	–

experiments [18,21,22]. In fact, the addition of water to an unsaturated lamellar system enlarges the dimension of the unit cell, as the amount of water between the lipid layers increases. If the projected electron density of the bilayer remains constant with swelling, the proper scaled intensities, measured varying the water content, are expected to sample the squared Fourier transform of the structure. Then, the signs of each structure factor may be deduced observing the behaviour of the continuous transform close to the zeros of intensities [18,21]. Actually, inside a swelling series, the structure may be modified, but if changes are small and continuous, the structure factor signs can still be obtained with reasonable certainty [22].

In the present case, three series of swelling experiments were performed at 65°C for different pindolol contents, namely $R = 0$, $R = 0.1$ and $R = 0.5$. The experimental data are listed in Tabel III. The plot of the structure factors as a function of the reciprocal spacing S ($Å^{-1}$) is reported in Fig. 7. In particular, the amplitudes were normalised according to [23]:

$$\sum I(h) = d / d_{min}$$

where d is the observed lamellar repeat distance determined in each experiment and d_{min} is the corresponding value observed for the sample of the series containing the minimum quantity of water. From the curves in Fig. 7, the position of zeros can be easily inferred. It could be noticed that the smooth curves do not exactly correspond to the Fourier transform of the same constant structure. This indicates that the bilayer is changing its structure with swelling: as already proposed [21], the increased disorder of the lipid molecules at higher water contents could explain such a behaviour.

Once determined the signs of the structure factors, the electron density distributions were finally evaluated, and electron density maps traced (for data normalization * see also Ref. 22). A comparative analysis of the results obtained in the three series is presented in Fig. 8, where electron density profiles relative to samples in the more hydrated condition (i.e., close to the fully hydration) are reported. The more evident effect due to the presence of pindolol is the deepening of the electron density profile in the paraffinic chain region: the position of the low electron-dense terminal

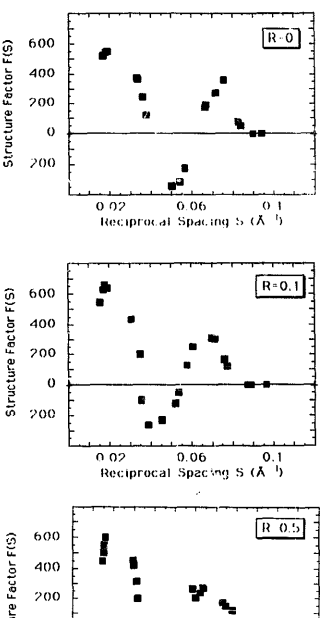

Fig. 7. Plot of the scaled structure factors observed in DSPC/water/pindolol mixtures at 65°C and at different degrees of swelling, as a function of the reciprocal spacings (see Table III). From top to bottom, the pindolol molar ratios ($R = mol_{pind} / mol_{DSPC}$) are: 0, 0.1 and 0.5.

methyl groups in fact appears more and more visible, confirming the proposed tightening of the hydrocarbon chain conformation. Moreover, it could be stressed that almost all drug effect is already present at $R = 0.1$, as not much difference seems to occur between the electron density profiles of $R = 0.1$ and $R = 0.5$ samples.

From the electron density maps, other information can be obtained, as it is possible to directly measure the dimension of the lipid and of the paraffinic layers

* In consequence of the data normalization, the electron density distribution ($\Delta\rho(r)$, also called the map) is a normalized dimensionless expression of the fluctuation of the electron density $\rho(r)$:

$$\Delta\rho(r) = [\rho(r) - \langle\rho\rangle] / [\langle\rho^2(r) - \langle\rho\rangle^2\rangle]^{1/2}$$

being $\rho(r)$ the Fourier transform of the set of observed structure factors and $\langle\rho\rangle$ the average value of $\rho(r)$ over the volume. See Ref. 22 and references therein.

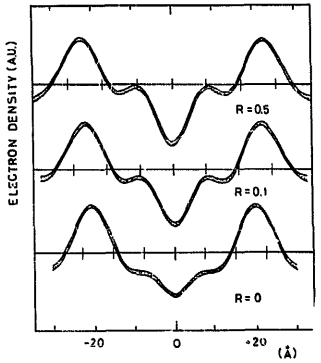

Fig. 8. Electron density profiles, obtained by Fourier transform of normalised structure factors (see Ref. 22), relative to the lamellar phase observed at maximum hydration at 65 °C in DSPC/water/pindolol mixtures. From top to bottom, the pindolol molar ratios ($R = mol_{pind}/mol_{DSPC}$) are: 0.5, 0.1 and 0. The origin is at the center of the hydrocarbon region. The dashed area represents the uncertainties in the electron density curves.

[22]. These data are reported in Table III: it could be noticed that the agreement between them and the corresponding values calculated from the chemical parameters is very good. In particular, the increase of the thickness of the lipid layer observed as a function of pindolol concentration appears directly confirmed.

5. Conclusions

Several conclusions can be derived from the above reports. First of all, the whole results show that pindolol determines structural modifications mainly at the paraffinic level of the model membrane, inducing a stiffening and tightening of the hydrocarbon chain arrangement. In the $L_{\beta'}$ and $P_{\beta'}$ phases, this appears as a decrease of the hydrocarbon chain tilt, while, at the higher drug content, a gel phase is induced: in this phase the chains are forced to completely interdigitate. Above the DSPC chain melting temperature, the pindolol effect persists, so that the chains assume a mixed 'disordered-ordered' conformation: a clear deepening of the electron density profile in correspondence of the paraffinic region is then observed in the calculated electron density maps. Noticeable is the fact that the drug modifies also the 'hydrophilic' properties of the membrane: in both $P_{\beta'}$ and $L_{\alpha\beta}$ phases, the pindolol increases the water content between the lipid layers.

The unusual phases induced by the pindolol appear more common then previously thought. In particular, gel phases have been observed in hydrated bilayers of dipalmitoylphosphatidylcholine at high concentration of glycerol or ethylene glycol [24] as well as of dipalmitoylphosphatidylglycerol after the addition of choline, acetylcholine and polymixine B [25,26]. More recently, it has been shown that several surface active small molecules (for example, drugs as tetracaine [16], chlorpromazine [16], azelaic acid [14], propanolol [5,27] and so on) but also uncharged compounds (as benzyl alcohol or phenylethanol [16]) can induce interdigitated phases. On the contrary, high temperature structural studies are relatively rare, so that the observation of a $L_{\alpha\beta}$ phase appears quite unusual.

On the basis of these considerations, a model relative to the lipid–pindolol interaction could be tentatively proposed. According to McIntosh et al. [16], it appears that all the molecules (either charged or neutral) just above considered, show amphiphilic properties, and tend to locate at the lipid/water interface. However, it has been observed that, to produce interdigitation, the added molecule must present some size constraints [5,16]; in particular, if the molecule leaves vacant places in the paraffinic region of the lipid bilayer, the chains can interpenetrate. Considering this picture, it is plausible that pindolol, anchoring at the interface, causes voids between lipid chains and then induces interdigitation. However, the effects observed in the $L_{\beta'}$ and $P_{\beta'}$ phases as well as the induction at high temperature of the $L_{\alpha\beta}$ phase, seem to indicate that the pindolol nonpolar moiety extends rather deeply into the bilayer interior, so that the hydrocarbon chains must adopt a different conformation. At low temperature, the loss of the required chemical homogeneity of the hydrocarbon moiety determines the observed gradual transition towards the untilted chain conformation. At high temperature, in order to satisfy the van der Waals interactions, the chains assume a mixed 'disordered-ordered' conformation. This behaviour could be related to the more general stabilizing effect observed in such kind of drugs.

Acknowledgements

It is a pleasure to thank Mr. Enzo Mosca for drawing the figures. A.C. acknowledges the ICTP (Trieste, Italy) for the financial support during her stay in Italy. This work was partially supported by the CNPq (Brazil) and CNR (Italy) exchange programs.

References

1 Filders, F.J.T. (1981) in Liposomes: from Physical Structure to Therapeutic Applications (Dingle, J.T. and Gordon, J.L., eds.), pp. 465–485, Elsevier/North Holland Biomedical Press, New York.

2 Cao, A., Hantz-Brachet, E., Azize, B., Taillandier, E. and Perret, G. (1991) Chem. Phys. Lip. 58, 225–232.
3 Hansch, C. and Clayton, J. (1973) J. Pharm. Sci. 62, 1–21.
4 Zimmer, G. (1984) in Biomembranes, Vol. 12 (Kates, M. and Manson, L.A., eds.), pp. 169–201, Plenum Press, New York.
5 Harish, M.P. and Ryman, B.E. (1981) in Liposomes: from Physical Structure to Therapeutic Applications (Dingle, J.T. and Gorden, J.L., eds.), pp. 409–441, Elsevier/North-Holland Biomedical Press, New York.
6 Schaerer, A.A. (1955) J. Am. Chem. Soc. 77, 2017–2024.
7 Tardieu, A. (1972) Thesis, Université Paris-Sud.
8 Stumpel, J., Eibl, H. and Nicksch, A. (1983) Biochim. Biophys. Acta 727, 246–254.
9 Blaurock, A.E. and Wilkins, M.H.F. (1969) Nature 223, 906–911.
10 Levine, Y.K. (1973) Progr. Surf. Sci. 3, 279–352.
11 Tardieu, A., Luzzati, V. and Reman, F.C. (1973) J. Mol. Biol. 75, 711–733.
12 Janiak, M.J., Small, D.M. and Shipley, G.G. (1976) Biochemistry 15, 4575–4580.
13 Luzzati, V. (1968) in Biological Membranes (Chapman, D., ed.), pp. 71–123, Academic Press, New York.
14 Bossi, G., Dubini, B., Mariani, P., Ponzi Bossi, M.G., Rustichelli, F. and Phadke, R.S. (1990) Il Nuovo Cimento 12D, 1293–1308.
15 Auger, M., Jarrel, H.C., Smith, I.C.P., Siminovitch, D.J., Mantsch, H. and Wong, P.T.T. (1988) Biochemistry 27, 6086–6093.
16 McIntosh, T.J., McDaniel, R.V. and Simon, S.A. (1983) Biochim. Biophys. Acta 731, 109–114.
17 Ranck, J.L., Mateu, L., Sadler, D.M., Tardieu, A., Gulik-Krzywicki, T. and Luzzati, V. (1974) J. Mol. Biol. 85, 249–277.
18 Lagguer, P. (1988) Top. Current Chem. 145, 174–202.
19 Bourges, M., Small, D.M. and Dervichian, D.G. (1967) Biochim. Biophys. Acta 137, 157–167.
20 International Tables for X-Ray Crystallography (1952) Vols. 1 and 2, The Kynoch Press, Birmingham.
21 Franks, N.P. (1976) J. Mol. Biol. 100, 345–358.
22 Mariani, P., Colotto, A. and Albertini, G. (1990) Chem. Phys. Lipids 55, 283–294.
23 Blaurock, A.E. (1971) J. Mol. Biol. 56, 35–52.
24 McDaniel, R.V., McIntosh, T.J. and Simon, S.A. (1982) Biochim. Biophys. Acta 731, 97–108.
25 Ranck, J.L. and Tocanne, J.F. (1982) FEBS Lett. 143, 171–174.
26 Ranck, J.L. and Tocanne, J.F. (1982) FEBS Lett. 143, 175–178.
27 Albertini, G., Donati, C., Phadke, R.S., Ponzi Bossi, M.G. and Rustichelli, F. (1990) Chem. Phys. Lipids 55, 331–337.